Title
Clinical Assessment of Deep Learning–based Super-Resolution for 3D Volumetric Brain MRI

Journal
Radiology Artificial Intelligence, 4(2)

ISSN
2638-6100

Authors
Rudie, Jeffrey D
Gleason, Tyler
Barkovich, Matthew J
et al.

Publication Date
2022-03-01

DOI
10.1148/ryai.210059

Peer reviewed

Radiology: Artificial Intelligence

AI IN BRIEF

Clinical Assessment of Deep Learning–based Super-Resolution for 3D Volumetric Brain MRI

Jeffrey D. Rudie, MD, PhD • Tyler Gleason, MD • Matthew J. Barkovich, MD • David M. Wilson, MD, PhD • Ajit Shankaranarayanan, PhD • Tao Zhang, PhD • Long Wang, PhD • Enhao Gong, PhD • Greg Zaharchuk, MD, PhD • Javier E. Villanueva-Meyer, MD

From the Department of Radiology & Biomedical Imaging, University of California, San Francisco, 505 Parnassus Ave, L-352, San Francisco, CA 94143 (J.D.R., T.G., M.J.B., D.M.W., J.E.V.M.); Subtle Medical, Menlo Park, Calif (A.S., T.Z., L.W., E.G.); and Department of Radiology, Stanford University, Stanford, Calif (G.Z.). Received February 27, 2021; revision requested March 29; revision received December 13; accepted December 23. **Address correspondence to** J.E.V.M. (e-mail: *javier.villanueva-meyer@ucsf.edu*).

Authors declared no funding for this work.

Conflicts of interest are listed at the end of this article.

Radiology: Artificial Intelligence 2022; 4(2):e210059 • https://doi.org/10.1148/ryai.210059 • Content codes: AI MR NR

Artificial intelligence (AI)–based image enhancement has the potential to reduce scan times while improving signal-to-noise ratio (SNR) and maintaining spatial resolution. This study prospectively evaluated AI-based image enhancement in 32 consecutive patients undergoing clinical brain MRI. Standard-of-care (SOC) three-dimensional (3D) T1 precontrast, 3D T2 fluid-attenuated inversion recovery, and 3D T1 postcontrast sequences were performed along with 45% faster versions of these sequences using half the number of phase-encoding steps. Images from the faster sequences were processed by a Food and Drug Administration–cleared AI-based image enhancement software for resolution enhancement. Four board-certified neuroradiologists scored the SOC and AI-enhanced image series independently on a five-point Likert scale for image SNR, anatomic conspicuity, overall image quality, imaging artifacts, and diagnostic confidence. While interrater κ was low to fair, the AI-enhanced scans were noninferior for all metrics and actually demonstrated a qualitative SNR improvement. Quantitative analyses showed that the AI software restored the high spatial resolution of small structures, such as the septum pellucidum. In conclusion, AI-based software can achieve noninferior image quality for 3D brain MRI sequences with a 45% scan time reduction, potentially improving the patient experience and scanner efficiency without sacrificing diagnostic quality.

Over the past several decades, MRI has become the key modality for brain imaging due to its excellent soft-tissue contrast. The main drawback remains relatively long image acquisition times. This problem has only been exacerbated by trends toward high resolution and volumetric acquisitions. Scan duration can be decreased through undersampling, but substantial undersampling leads to an ill-posed linear inverse reconstruction problem that is often beyond the capability of common acceleration methods such as parallel imaging (1) and compressed sensing (CS) (2). The lengthy reconstruction times for parallel imaging and CS under moderate acceleration are also not ideal in the clinical setting.

Deep learning, a form of supervised machine learning, has the potential to mitigate the trade-offs between scan quality and acquisition times, either by shortening the acquisition time for a given MRI sequence or by improving image quality of a given sequence without lengthening acquisition time (3–6). Additionally, despite the greater adoption of 3-T imaging, 1.5-T scanners, with lower signal-to-noise ratio (SNR), remain prevalent in clinical practice. Deep learning has the potential to improve image quality at 1.5 T by improving the signal-to-noise per unit time without incurring worse susceptibility artifacts or increased patient heating that can be seen at higher field strengths such as 3 T. For example, use of deep learning–based denoising and SNR enhancement algorithms has already been demonstrated for various structural MRI applications, including postcontrast MRI with reduced gadolinium dose (7), the reconstruction of 7-T–like images from 3-T MRI (8), and reconstruction of multicontrast MR images (9). A recent study showed that image quality and quantitative volumetric information at T1 imaging is maintained on artificial intelligence (AI)–enhanced fast scans when morphologic postprocessing is applied (10). However, to our knowledge, little work has been done to evaluate this method in clinical practice on multimodal MRI studies of clinical patients with lesions.

The purpose of this study was to qualitatively evaluate brain MRI quality using a commercially available deep learning–based denoising and resolution enhancement algorithm to reduce scan time while preserving image quality and spatial resolution of small structures of three-dimensional (3D) T2 fluid-attenuated inversion recovery (FLAIR), 3D T1 precontrast, and 3D T1 postcontrast images.

Materials and Methods

Image Acquisition and Enhancement

In this prospective study, 32 consecutive patients undergoing clinical brain MRI with a 1.5-T Signa HDxt scanner (GE Healthcare) at the University of Southern California San Francisco Medical Center were recruited for this study. The study was part of a quality improvement project that did not require consent and included the minimum number of patients needed to assess quality by the institution. Twenty-five patients were undergoing posttreatment brain tumor assessment, six patients were undergoing workup for headaches, and one patient was

Abbreviations

AI = artificial intelligence, CS = compressed sensing, FDA = Food and Drug Administration, FLAIR = fluid-attenuated inversion recovery, FWHM = full-width half maximum, SNR = signal-to-noise ratio, SOC = standard of care, 3D = three dimensional

Summary

An artificial intelligence–based software for super-resolution was prospectively evaluated on three-dimensional brain MRI sequences performed for routine clinical patients, showing noninferior image quality with a 45% scan time reduction.

Key Points

- Artificial intelligence (AI)–enhanced scans were noninferior for all qualitative metrics including image signal-to-noise ratio (SNR), anatomic conspicuity, overall image quality, imaging artifacts, and diagnostic confidence and actually demonstrated a qualitative SNR improvement.
- Quantitative analyses demonstrated that AI-enhanced faster low-resolution images improved spatial resolution of the septum pellucidum compared with original fast-acquisition scans, approaching the spatial resolution of the standard-of-care scans.

Keywords

MR Imaging, CNS, Brain/Brain Stem, Reconstruction Algorithms

undergoing assessment for cognitive dysfunction. In addition to the institute's standard of care (SOC) routine brain tumor protocols that included 3D T1 precontrast, 3D T2 FLAIR, and 3D T1 postcontrast pulse sequences (with parallel imaging factor of two using array spatial sensitivity encoding technique [ie, ASSET; GE Healthcare]), a faster version of these sequences was performed for all patients, with half of the number of phase-encode lines as the SOC scans, resulting in reduced in-plane spatial resolution (256 × 128 instead of 256 × 256; full details of the SOC and faster MRI acquisition parameters are in Table 1). The fast scans were performed immediately after each SOC sequence. The corresponding scan times with SOC and faster sequences were 2 minutes 55 seconds and 1 minute 36 seconds for 3D T1 pre- and postcontrast studies, and 5 minutes 44 seconds and 3 minutes 10 seconds for 3D T2 FLAIR, respectively. This corresponded to reductions of approximately 45% in scan time, leading to a total time savings of 5 minutes 12 seconds for these three acquisitions. Three of the 32 patients underwent noncontrast MRI examinations; in these patients, only the 3D T1 precontrast and 3D T2 FLAIR sequences were performed. Gadoterate meglumine (Dotarem; Guerbet) was used as contrast agent and administered using hand injection.

A Food and Drug Administration (FDA)–cleared, commercially available AI-based image enhancement software (SubtleMR version 1.2; Subtle Medical; 510 K clearance K191688) was applied to the faster sequences to improve image resolution. This algorithm is based on a U-Net deep convolutional neural network backbone that was previously trained on a large number of paired low- and high-resolution images acquired from a variety of vendors, field strengths, and institutions. A new series with the same nominal resolution as the SOC sequence was generated after applying the AI-enhanced algorithm. Both the SOC images and AI-enhanced processed images were evaluated. A total of 186 images (93 each from SOC and AI-enhanced, consisting of pairs of 64 T1 precontrast, 64 T2 FLAIR, and 58 T1 postcontrast) were included in this study.

Subtle Medical provided access to the deep learning software product at no cost. Several of the authors of the study are Subtle Medical employees and assisted with the statistical tests. They did not have control over the patients selected in the study, the analysis approach, or the information submitted for publication.

Qualitative Analyses

Four board-certified neuroradiologists (D.W.M., J.E.V.M., M.J.B., and J.D.R., with 10, 5, 2, and 1 year(s) post–neuroradiology fellowship experience, respectively) independently evaluated the 186-image series on their personal computers using OsiriX, which allows standard window and level adjustments, without proctoring. The images were de-identified for technique and patient and randomized. Each image series

Table 1: Imaging Acquisition Parameters

	Sequence					
	3D T1 Precontrast		3D T2 FLAIR		3D T1 Postcontrast	
Imaging Parameter	SOC	Faster	SOC	Faster	SOC	Faster
Acquisition plane	Axial	Axial	Sagittal	Sagittal	Axial	Axial
TR (msec)	8	8	5500	5500	8	8
TE (msec)	3	3	160	160	3	3
Flip angle (degrees)	15	15	90	90	15	15
Section thickness (mm)	1.4	1.4	1.4	1.4	1.4	1.4
Acquisition matrix	256 × 256	256 × 128	256 × 256	256 × 128	256 × 256	256 × 128
Acquisition time (sec)	175	96	344	190	175	96
Time reduction (%)		45.1		44.7		45.1

Note.—Acquisition parameters of the standard of care (SOC) and faster three-dimensional (3D) T1 precontrast, 3D T2 fluid-attenuated inversion recovery (FLAIR), and 3D T1 postcontrast images. TE = echo time, TR = repetition time.

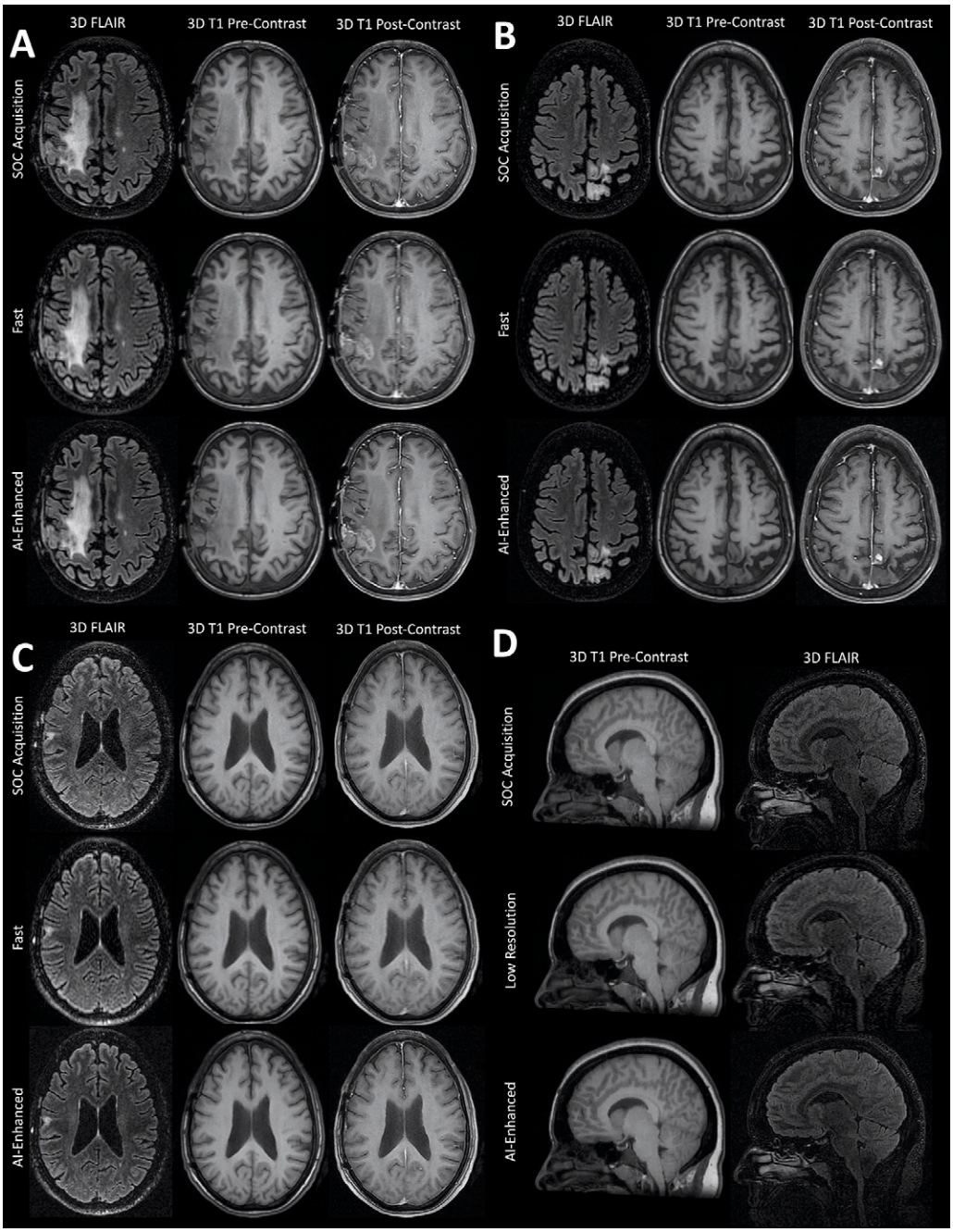

Figure 1: Example clinical MRI studies. **(A–C)** Three example axial three-dimensional (3D) fluid-attenuated inversion recovery (FLAIR) (first column), 3D T1 precontrast (second column), and 3D T1 postcontrast (third column) images from standard-of-care (SOC) acquisition (first row), low-resolution fast-acquisition (second row), and artificial intelligence (AI)–enhanced (third row) images in three patients being evaluated for follow-up of diffuse gliomas. **(D)** Example sagittal 3D T1 precontrast (first column) 3D FLAIR (second column), SOC acquisition (first row), low-resolution fast-acquisition (second row), and AI-enhanced (third row) images in a patient with headaches, determined to have intracranial hypotension.

was rated on a subjective five-point Likert scale (1 = nondiagnostic, 2 = poor, 3 = acceptable, 4 = good, 5 = excellent) for the following criteria: *(a)* image SNR, *(b)* anatomic conspicuity, *(c)* overall image quality, *(d)* imaging artifacts, and *(e)* diagnostic confidence. Wilcoxon rank sum tests with a 0.25-point noninferiority threshold were performed to assess whether noninferior image quality was achieved by using the AI-enhanced scans when compared with SOC scans. Interreader variability was assessed using the weighted κ statistic. This was done for each of the contrast types (3D T2 FLAIR, 3D T1 precontrast, and 3D T1 postcontrast) for each of the pairs of raters.

Quantitative Analyses

To quantitatively demonstrate the increased spatial resolution between the faster sequence and AI-enhanced images, measurements of the apparent full-width half maximum (FWHM) of the septum pellucidum in the axial plane were

performed by two independent researchers blinded to the type of image being assessed. The apparent FWHM measurement was calculated on the generated histograms by measuring the difference between the two values of the voxel location that were half the maximum of the signal intensity. The human septum pellucidum is a hair-thin structure that is 1 mm or less in width in 54% of patients and less than 2 mm in an additional 11%–16% of patients (11). Therefore, a lower FWHM is a measure of the performance of the super-resolution algorithm. Paired *t* tests were used to compare septum pellucidum FWHM for SOC, fast, and AI-enhanced T1 precontrast images with statistical significance defined at the $\alpha = .05$ level.

Table 2: Multirater Qualitative Assessments

Rating Criterion for Each Sequence	Image Type		
	SOC	AI-enhanced	*P* Value
3D T1 precontrast			
Overall	4.0 ± 0.7	4.1 ± 0.7	<.001
SNR	3.6 ± 0.6	4.0 ± 0.8	<.001
Conspicuity	4.1 ± 0.7	4.1 ± 0.6	.41
IQ	3.9 ± 0.8	4.0 ± 0.8	.20
Artifact	4.2 ± 0.7	4.3 ± 0.7	.18
DC	4.2 ± 0.7	4.3 ± 0.7	.20
3D T2 FLAIR			
Overall	4.1 ± 0.8	4.2 ± 0.7	<.001
SNR	3.7 ± 0.8	4.1 ± 0.7	<.001
Conspicuity	4.2 ± 0.7	4.3 ± 0.6	.05
IQ	4.0 ± 0.8	4.1 ± 0.8	.04
Artifact	4.3 ± 0.7	4.4 ± 0.7	≤.02
DC	4.3 ± 0.7	4.3 ± 0.6	.26
3D T1 postcontrast			
Overall	4.0 ± 0.7	3.9 ± 0.7	.99
SNR	3.8 ± 0.7	4.0 ± 0.6	.02
Conspicuity	4.2 ± 0.6	3.9 ± 0.6	.99
IQ	4.0 ± 0.7	3.7 ± 0.7	.99
Artifact	4.0 ± 0.7	3.9 ± 0.9	.80
DC	4.2 ± 0.7	4.0 ± 0.8	.99

Note.—Data are the average ± standard deviation rater scores of the standard-of-care (SOC) and artificial intelligence (AI)–enhanced three-dimensional (3D) T1 precontrast, 3D T2 fluid-attenuated inversion recovery (FLAIR), and 3D T1 postcontrast images using a five-point Likert scale (1 = nondiagnostic, 2 = poor, 3 = acceptable, 4 = good, 5 = excellent) for the following criteria: image signal-to-noise ratio (SNR), anatomic conspicuity, overall image quality (IQ), imaging artifacts, and diagnostic confidence (DC). Statistical comparisons of rater scores were made using paired Wilcoxon rank sum tests.

Results

Qualitative Results

Representative examples of the SOC, faster, and AI-enhanced images are shown in Figure 1A–1D. The average scores for image SNR, anatomic conspicuity, overall image quality, imaging artifacts, and diagnostic confidence are shown in Table 2. None of the studies were rated as nondiagnostic for any of these categories. For both the T1 pre- and postcontrast sequences, the AI-enhanced images received statistically significantly higher ratings than the SOC images for image SNR. For other metrics, the T1 postcontrast SOC images were slightly preferred to the AI-enhanced images. For the T2 FLAIR images, the AI-enhanced images received statistically significantly higher ratings than the SOC images in all criteria except diagnostic confidence. The hypothesis that the AI-enhanced fast images were noninferior to the standard scan was not rejected ($P > .05$) for any evaluation metric for any of the sequences. The κ scores among the four readers showed low to fair agreement (Table 3).

Quantitative Results

The FWHM of the septum pellucidum on the fast and AI-enhanced fast images for 3D T1 precontrast by two independent raters were as follows: SOC, 1.65 mm ± 0.25 (standard deviation) and 1.64 mm ± 0.42; fast, 2.58 mm ± 0.24 and 2.70 mm ± 0.39; AI-enhanced fast, 1.79 mm ± 0.26 and 1.98 mm ± 0.39, respectively, over 32 cases ($P < .001$ for comparison between fast and AI-enhanced fast; $P = .06$ and $P = .007$ for comparison between SOC and AI-enhanced). Examples of the FWMH measurements are shown in Figure 2.

Discussion

In this study, we qualitatively and quantitatively evaluated an FDA-approved super-resolution AI-based image enhancement software to accelerate sequences with a 45% scan time reduction in a realistic clinical setting. We found noninferior qualitative assessments compared with existing standard duration sequences as assessed with multiple image quality metrics by four experienced academic neuroradiologists. In addition, spatial resolution of small structures was improved compared with the original fast-acquisition scans, approaching spatial resolution of the SOC scans.

While AI methods have been shown to improve image quality for a host of different structural MRI applications (7–9), it is important to determine whether they generalize beyond an individual scanner or practice setting, given that many AI algorithms have shown poorer performance when applied to external test sets (12). Furthermore, these cases were collected in a prospective consecutive manner, mimicking how the algorithm might be used in clinical practice. Using a strict noninferiority threshold of 0.25 point on a five-point Likert scale, none of the AI-enhanced sequences were found inferior to the standard longer sequences. For several of the criteria, particularly for perceived image SNR and imaging artifacts, the AI-enhanced studies were rated significantly higher. This may be related to two factors. First, because the algorithm has trained on a large

Table 3: Interrater Agreement

Image Type	Reader A	Reader B	κ Score
T1 precontrast	Rater 1	Rater 2	0.28
	Rater 1	Rater 3	0.26
	Rater 1	Rater 4	0.27
	Rater 2	Rater 3	0.10
	Rater 2	Rater 4	0.16
	Rater 3	Rater 4	0.22
T2 FLAIR			
	Rater 1	Rater 2	0.22
	Rater 1	Rater 3	0.47
	Rater 1	Rater 4	0.25
	Rater 2	Rater 3	0.14
	Rater 2	Rater 4	0.04
	Rater 3	Rater 4	0.27
T1 postcontrast			
	Rater 1	Rater 2	−0.03
	Rater 1	Rater 3	0.26
	Rater 1	Rater 4	0.24
	Rater 2	Rater 3	0.09
	Rater 2	Rater 4	0.24
	Rater 3	Rater 4	0.30

Note.—The κ scores for all possible pairs of raters for all three-dimensional (3D) T1 precontrast, 3D T2 fluid-attenuated inversion recovery (FLAIR), and 3D T1 postcontrast images.

number of diverse cases, there is a denoising effect in addition to the designed super-resolution. Second, shorter acquisition times may reduce the opportunity for patient motion–related artifacts. Faster scans may also have a substantial impact on patient satisfaction and tolerance of MRI, given that up to 30% of patients report anxiety during an MRI examination, mostly due to claustrophobia (13). We emphasize that no quantitative SNR measurements were made, as the algorithm was designed to simulate as much as possible the SOC high-resolution images, including their SNR profile. The perception of higher SNR for the AI-enhanced studies is based solely on subjective evaluation by the radiologist readers.

While we believe multireader studies by experienced radiologists are still the best way to test a new algorithm, given the need to synthesize many aspects of image quality into a diagnostic assessment, we also performed a quantitative test to demonstrate the improved resolution of the AI-enhanced images. The septum pellucidum, typically beyond the spatial resolution of most MRI sequences (11), provides a good test of true image resolution. In our study, we found that applying the AI algorithm to the faster sequences led to a reduced apparent thickness as measured by the FWHM relative to the fast low-resolution scans, closer but slightly lower than the SOC scans. A recent complementary study found that analyses of AI-enhanced and SOC T1 images provided equivalent quantitative volumetric information (10). These findings support the qualitative evaluation of four

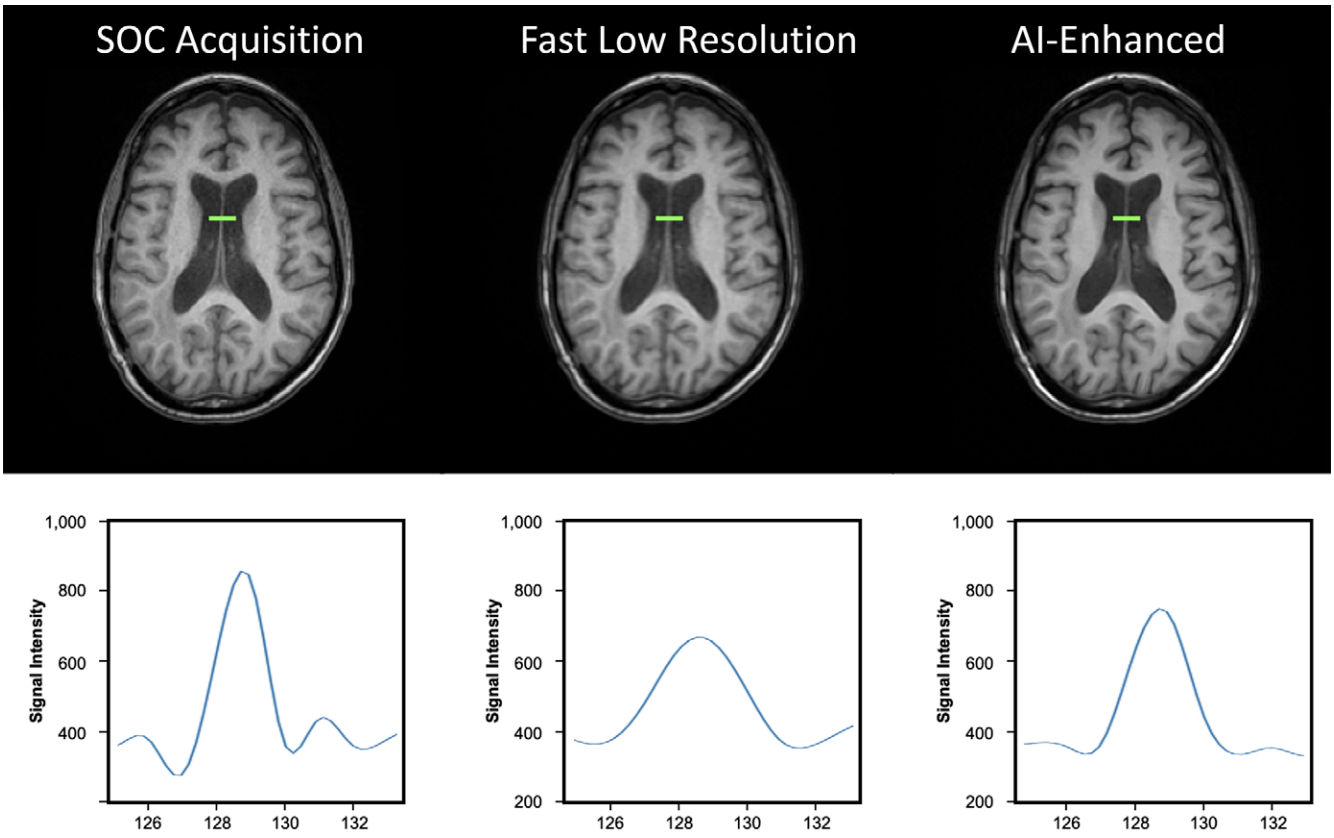

Figure 2: Septum pellucidum measurements. Example axial three-dimensional T1 precontrast images from standard-of-care (SOC) acquisition (left), low resolution, fast acquisition (middle), and artificial intelligence (AI)–enhanced (right) and example histograms of the apparent full-width half maximum of the septum pellucidum in the axial plane. Green bar represents site of sampling for the full-width half maximum measurements of the septum pellucidum depicted in each graph.

experienced neuroradiologists that the images produced by the AI method when applied to fast scans are diagnostically equivalent to the standard, longer 3D sequences.

There were several limitations to the current study. The first was the relatively small sample size with relatively limited pathologic types scanned with the same 1.5-T clinical scanner. Future evaluations at multiple sites and in larger patient cohorts should be performed. This is especially true for small lesions, as there are some concerns that information could be lost in deep learning reconstruction (14). However, a recent empirical study found that deep learning–based reconstruction methods are quite robust to minimal perturbations and are good at accurately recovering fine details (15). While there was no subjective difference in diagnostic quality observed in this initial prospective study, it did not encompass the full spectrum of lesions encountered in clinical practice, including smaller and more subtle lesions, thus it will be important to evaluate smaller lesions such as sub-3-mm brain metastases in future studies. Overall, our results suggest that studies involving high-resolution 3D imaging could be significantly shortened using AI methods, improving the patient experience and scanner efficiency and reducing costs for patients and health care networks without sacrificing diagnostic quality.

Author contributions: Guarantors of integrity of entire study, **E.G.**, **J.E.V.M.**; study concepts/study design or data acquisition or data analysis/interpretation, all authors; manuscript drafting or manuscript revision for important intellectual content, all authors; approval of final version of submitted manuscript, all authors; agrees to ensure any questions related to the work are appropriately resolved, all authors; literature research, **J.D.R.**, **T.G.**, **D.M.W.**, **E.G.**, **G.Z.**, **J.E.V.M.**; clinical studies, **J.D.R.**, **T.G.**, **M.J.B.**, **T.Z.**, **L.W.**, **E.G.**, **G.Z.**, **J.E.V.M.**; statistical analysis, **A.S.**, **E.G.**, **G.Z.**; and manuscript editing, **J.D.R.**, **T.G.**, **M.J.B.**, **D.M.W.**, **A.S.**, **T.Z.**, **E.G.**, **G.Z.**, **J.E.V.M.**

Disclosures of conflicts of interest: **J.D.R.** American Society of Neuroradiology Research Grant in Artificial Intelligence; alum of *Radiology: Artificial Intelligence* Trainee Editorial Board (2019-2021). **T.G.** No relevant relationships. **M.J.B.** No relevant relationships. **D.M.W.** No relevant relationships. **A.S.** Employee of Subtle Medical; stock options in Subtle Medical. **T.Z.** Grant support from Subtle Medical, National Institutes of Health (NIH), Small Business Innovation Research (grant R44EB027560); support for attending meetings from Subtle Medical and NIH; patents planned, issued, or pending with Subtle Medical; stock or stock options in Subtle Medical. **L.W.** Employee of Subtle Medical; stocks from Subtle Medical. **E.G.** Stock or stock options with Subtle Medical. **G.Z.** Co-founder of Subtle Medical; multiple NIH grants to institution; grants from GE Healthcare; royalties or licenses from Cambridge University Press; various patents on deep learning to author and institution; payment or honoraria from Biogen (advisory board) and Asia-Oceanian Congress of Neuroradiology and Asian Oceanian Congress of Neurology (honoraria); payment from various law firms for expert testimony; support for meeting attendance or travel from Subtle Medical to attend British Institute of Radiology 2020; multiple planned, pending, and issued patents to author and institution; member of International Society for Magnetic Resonance in Medicine board of trustees (no payment); stock or stock options in Subtle Medical; institution received equipment from NVIDIA (GPU donation program). **J.E.V.M.** No relevant relationships.

References

1. Hamilton J, Franson D, Seiberlich N. Recent advances in parallel imaging for MRI. Prog Nucl Magn Reson Spectrosc 2017;101:71–95.
2. Ye JC. Compressed sensing MRI: a review from signal processing perspective. BMC Biomed Eng 2019;1(1):8.
3. Pham CH, Ducournau A, Fablet R, Rousseau F. Brain MRI super-resolution using deep 3D convolutional networks. In: 2017 IEEE 14th International Symposium on Biomedical Imaging (ISBI 2017), Melbourne, Australia, April 18–21, 2017. Piscataway, NJ: IEEE, 2017; 197–200.
4. Mardani M, Gong E, Cheng JY, et al. Deep Generative Adversarial Neural Networks for Compressive Sensing MRI. IEEE Trans Med Imaging 2019;38(1):167–179.
5. McCann MT, Jin KH, Unser M. Convolutional Neural Networks for Inverse Problems in Imaging: A Review. IEEE Signal Process Mag 2017;34(6):85–95.
6. Chaudhari AS, Fang Z, Kogan F, et al. Super-resolution musculoskeletal MRI using deep learning. Magn Reson Med 2018;80(5):2139–2154.
7. Gong E, Pauly JM, Wintermark M, Zaharchuk G. Deep learning enables reduced gadolinium dose for contrast-enhanced brain MRI. J Magn Reson Imaging 2018;48(2):330–340.
8. Bahrami K, Shi F, Zong X, Shin HW, An H, Shen D. Reconstruction of 7T-Like Images From 3T MRI. IEEE Trans Med Imaging 2016;35(9):2085–2097.
9. Do W-J, Seo S, Han Y, Ye JC, Choi SH, Park S-H. Reconstruction of multicontrast MR images through deep learning. Med Phys 2020;47(3):983–997.
10. Bash S, Wang L, Airriess C, et al. Deep Learning Enables 60% Accelerated Volumetric Brain MRI While Preserving Quantitative Performance: A Prospective, Multicenter, Multireader Trial. AJNR Am J Neuroradiol 2021;42(12):2130–2137.
11. Schunk H. Congenital dilatations of the septum pellucidum. Radiology 1963;81(4):610–618.
12. Zech JR, Badgeley MA, Liu M, Costa AB, Titano JJ, Oermann EK. Variable generalization performance of a deep learning model to detect pneumonia in chest radiographs: A cross-sectional study. PLoS Med 2018;15(11):e1002683.
13. Meléndez JC, McCrank E. Anxiety-related reactions associated with magnetic resonance imaging examinations. JAMA 1993;270(6):745–747.
14. Antun V, Renna F, Poon C, Adcock B, Hansen AC. On instabilities of deep learning in image reconstruction and the potential costs of AI. Proc Natl Acad Sci U S A 2020;117(48):30088–30095.
15. Darestani MZ, Chaudhari AS, Heckel R. Measuring Robustness in Deep Learning Based Compressive Sensing. arXiv:2102.06103 [preprint] http://arxiv.org/abs/2102.06103. Posted February 11, 2021. Accessed September 13, 2021.